Polarization-Independent All-Wave Polymer-Based TIR Thermooptic Switch

Xiaolong Wang, Brie Howley, Maggie Y. Chen, *Member, IEEE*, and Ray T. Chen, *Fellow, IEEE*

***Abstract*—The optimal design of a polymer-based thermooptic (TO) switch using a total internal reflection (TIR) effect is proposed to improve switching performance. Numerical calculations show that this type of optical switch can achieve an ultrabroad optical bandwidth as well as a low polarization dependent loss. The devices fabricated with different half branch angles consume driving powers from 25 to 66 mW. The switches also show fiber-to-fiber insertion losses at 2.8 dB and polarization dependent losses (PDLs) at 0.2 dB. The measured rising and falling times are 1.5 and 2 ms, respectively. The optical bandwidth of the devices, which is limited by the material absorption from the fluorinated polymer, is quite large extending from 630 to 1630 nm.**

***Index Terms*—Optical switch, polymer waveguide, thermooptic (TO) effect, total internal reflection (TIR).**

I. Introduction

OPTICAL switches are important elements in many applications, such as optical add-drop multiplexing (OADM), optical cross connect (OXC) [1], and optical true time delay (TTD) [2], [3]. Benefiting from planar lightwave circuit (PLC) technologies, optical switches can be integrated on a single chip with many other devices including array waveguide gratings (AWG), optical couplers/splitters, variable optical attenuators (VOA), and optical delay lines. These applications require the optical switch to be wavelength insensitive as well as polarization independent to enhance the system transmit capacity.

Polymers are an ideal choice for such an integration platform. This low-cost material can be easily manipulated by methods such as molding, sawing, and dry etching [4]. Additionally, polymers have a large polarization independent thermooptic (TO) effect, which is one order greater than that of silica. In spite of a relatively slower response compared to electrooptic devices, the simpler fabrication procedure and more reliable performance of TO devices have kept them popular and commercially available in recent years.

The TO effect of polymeric materials is negative, i.e., the refractive index of the polymer decreases as the temperature rises. Thus, a total internal reflection (TIR) optical switch can be formed if a heater is set at the crossing point of a symmetric X junction [5]–[7]. Compared with various TO switch configurations, such as a digital optical switch (DOS) [8], a Mach–Zehnder interferometer (MZI) switch [9], or a directional coupler switch [10], TIR switches have a significant advantage in their broad optical bandwidth (or equivalently, their wavelength insensitivity). In this paper, 2×2 switches using the TIR effect are designed and fabricated. The minimum effective length of the device is only 3731 μm with the optimal design. Experimental results show that the working wavelength can extend from 630 to 1630 nm with power consumptions from 25 to 66 mW for different devices.

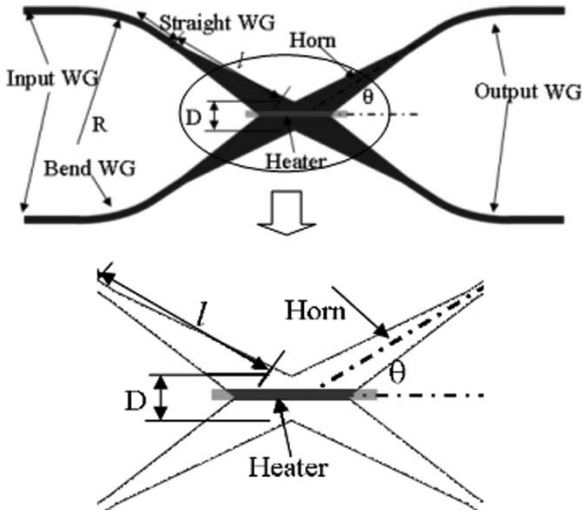

Fig. 1. Schematic diagram of the TO TIR switch.

II. Design

The design of a TIR TO switch deals with two major issues: optical and thermal characteristics. Some general concepts are discussed in [7]. Fig. 1 shows the schematic diagram of the TO TIR switch. The refractive indexes of the cladding and core used in the simulation are 1.45 and 1.46, respectively, corresponding to the actual materials used. The waveguide dimension is 6.5×6.5 μm^2. The separation of the input/output waveguide is 250 μm, which is compatible with a standard fiber array. The radii (R) of the bend waveguides are fixed at 10 mm, which is large enough such that negligible bending loss and guided mode perturbation result. The bend waveguides are then connected by two straight waveguides to form an X junction. Horn structures are introduced near the junction area for two purposes: to reduce the crosstalk and to make it compatible with the temperature gradient. The electrode heater, formed by a thin layer of gold film, is shortened and narrowed to reduce the power consumption compared with [6]. The electrode heater is connected to two enlarged pads by tapered lead lines. With

Manuscript received May 26, 2005; revised November 21, 2005.

X. Wang, B. Howley, and R. T. Chen are with the Microelectronics Research Center, University of Texas at Austin, Austin, TX 78758 USA (e-mail: wangxl@mail.utexas.edu; brie@ece.utexas.edu; raychen@uts.cc.utexas.edu).

M. Y. Chen is with the Omega Optics, Austin, TX 78758 USA (e-mail: maggie.chen@eomegaoptics.com).

Digital Object Identifier 10.1109/JLT.2005.863236

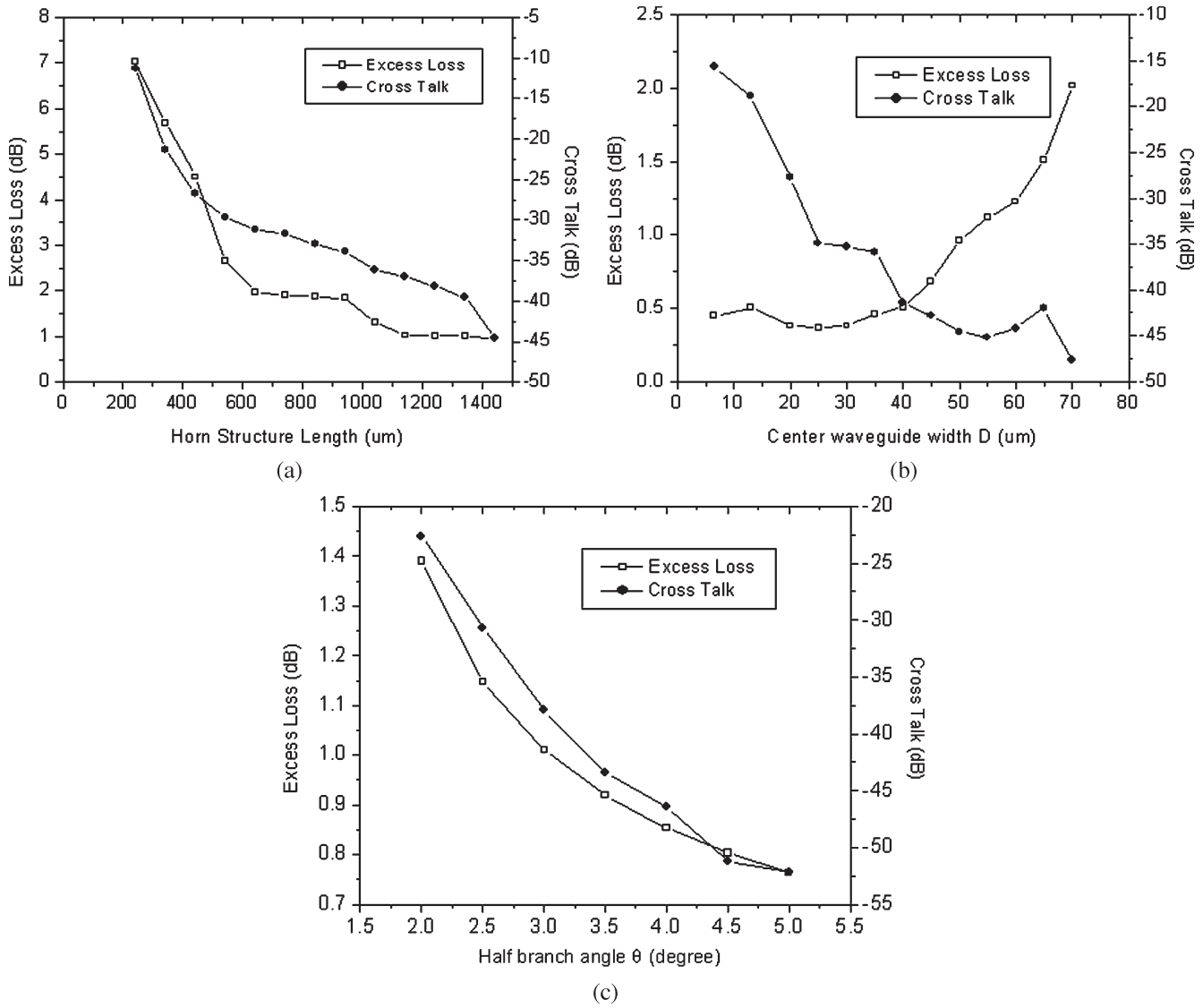

Fig. 2. Excess loss and crosstalk as functions of (a) horn structure length, (b) junction width, and (c) half branch angle.

this structure, the lead resistance can be reduced and the heating efficiency can be improved.

A. Optical Optimization of the X Junction

To improve the performance of the switches, the paramount concern is the geometric parameters of the X junction. Three-dimensional semi-vector beam propagation method (3-D SV BPM) [11] is employed in this investigation. If the half branch angle of the junction is θ, the effective length of the switch, namely, the total device length excluding the input/output waveguides, is determined by

$$L = 2\left\{\frac{\left[\frac{P}{2} - R(1-\cos\theta)\right]}{\tan\theta} + R\sin\theta\right\}. \tag{1}$$

The length of the horn structure l can vary from 0 to $l_{\max}$, where

$$l_{\max} = \frac{\left[\frac{P}{2} - R(1-\cos\theta)\right]}{\sin\theta}. \tag{2}$$

The most critical parameters are the taper length l, the junction width D, and the half branch angle θ. In order to optimize these three parameters, two of them are fixed, and the third is determined. All simulations in this paper are based on the TE mode. Since both the switch structure and the TO effect are polarization independent, the TM mode shows the same behavior as the TE mode.

First, D and θ are set at 50 μm and 4° based on our previous experimental result to determine l. Fig. 2(a) shows the excess loss and crosstalk as functions of l. Excess loss represents the loss caused by the switch structure excluding the coupling loss, material absorption, and Fresnel reflections. The simulation result in Fig. 2(a) shows that longer l leads to lower excess loss and lower crosstalk. For example, at the maximum length, where $l_{\max} = 1442$ μm, the excess loss is 0.96 dB, and the crosstalk is below -44 dB. In later simulations, $l = l_{\max}$ will be adopted. A direct explanation for this result is that longer taper length causes smoother adiabatic mode transformation from the straight waveguide to the horn structure [12]. Fig. 2(b) shows the excess loss and crosstalk as functions of D, when

$l = 1442$ μm and $\theta = 4^\circ$. A compromise has to be made to obtain a low excess loss as well as low crosstalk. We conclude based on the simulation that 40–50 μm is a good range because it also fits the requirement of the temperature gradient, which will be discussed in Section II-B. Fig. 2(c) shows the variation of the excess loss and crosstalk with θ. With the increase of θ, both the excess loss and crosstalk will decrease. However, with the increase of θ, more driving power has to be applied to switch the light, which will eventually burn the device. Thermal simulations show that if $\theta > 6^\circ$, the electrode heater temperature has to be greater than 251 °C.

B. Thermal State in the Active Region

The heating structure shown in Fig. 1 is quite similar to the model in [13]. The temperature of the electrode heater, which can be considered to be infinitely long compared with the electrode width, was given in [13]

$$T = T_{\mathrm{a}} + \frac{J^2 \rho_0}{\frac{K_{\mathrm{i}}}{t t_{\mathrm{i}}}\left[1 + \frac{0.88 t_{\mathrm{i}}}{w}\right] - J^2 \rho_0 \beta} \tag{3}$$

where T_{a} is the ambient temperature, J is the current density, ρ_0 is the resistivity of the metal, β is the temperature coefficient of the resistivity (ignored here), t is the metal thickness, w is the metal linewidth, and K_{i} is the thermal conductivity of the polymer. The density of the polymer used in this paper is $\rho = 1.0$ g/cm^3, the specific heat is $c = 0.84$ J/g $\cdot$ K, and the thermal conductivity is $K = 2 \times 10^{-3}$ W/cm $\cdot$ K. Equation (3) can then be written in a simpler form

$$T = T_{\mathrm{a}} + \frac{\frac{P_0}{l_{\mathrm{ele}}}}{K_{\mathrm{i}}\left(\frac{w}{t_{\mathrm{i}}} + 0.88\right)} \tag{4}$$

where P_0 is the heating power, and l_{ele} is the length of the electrode heater. Equations (3) and (4) are only valid if $l_{\mathrm{ele}} \gg w$, which allows the two-dimensional (2-D) model approximation. The case under here consideration is $P_0 =$ 44 mW, $l_{\mathrm{ele}} = 1500$ μm, $w = 8$ μm, $t_{\mathrm{i}} = 18$ μm, $T_{\mathrm{a}} = 25$ °C, resulting in a $T = 125.6$ °C. This case corresponds to the fabricated device discussed in Section IV.

However, what we are most concerned with is the temperature of the polymer rather than the electrode heater. Thus, numerical simulations using the finite element analysis (FEA) method have to be carried out to solve the 2-D thermal conduction equation. Fig. 3(a) shows the three-layer active region that will be analyzed. The geometry is simplified by approximating the central convex waveguide as a planar layer, since we use a thick top cladding (> 8 μm) to reduce metal absorption and since the junction width is significantly greater than the temperature extension width (TEW). The parameters used to calculate the steady-state temperature distribution are the same condition as given above. The temperature at the electrode heater is 131 °C, which is close to the temperature derived by (4). The simulation also indicates that along the mid-height of the core, the temperature resembles a Gaussian distribution. Fig. 3(b) shows the temperature distribution for various w, demonstrating that narrower electrode heater widths will lead to higher central waveguide temperatures and steeper temperature gradients, especially in the region right below the electrode heater. We define the TEW as the distance to the waveguide center where ΔT is half of the maximum ΔT. A smaller TEW represents a better heat confinement and higher heating efficiency. Otherwise, for a given change of the refractive index, a smaller width will require less driving power. However, some fabrication issues limit the narrowness of the electrodes. Since $w = 8$ μm does not yield a significant improvement over 2 μm, $w = 8$ μm is adopted in the real fabrication.

Fig. 4(a) shows the transient temperature response of the electrode heater and central waveguide. We define t_{rise} as the time from 0% to 90% $\Delta T_{\max}$ and t_{fall} as from $\Delta T_{\max}$ to 10% $\Delta T_{\max}$. The simulated t_{rise} and t_{fall} are 1.0 and 1.1 ms, respectively, which are also the switching times for the TIR switch. The polymer thickness t_{i} has significant impact on the switching time. If the polymer thickness is decreased, the heat can easily go through the polymer film to the silicon wafer, which is a good thermal conductor, thus achieving a higher speed. However, the switch will also consume more driving power with a decrease in t_{i}. Fig. 4(b) shows how the switching time and the power consumption vary with t_{i}. From this chart, we conclude that for a TIR switch with a half branch angle of 4°, the power consumption cannot be less than 38 mW, which is determined by the heat sinking rate of the polymer. The switching time cannot go below 5 μs, being limited by the thermal response of the silicon wafer. Although we can make a TO switch with a switching time less than 10 μs if $t_{\mathrm{i}} < 1$ μm, the optical loss will become intolerable due to the low coupling efficiency and the large metal and substrate absorption.

C. Reflection at the X Junction

One possible approach to evaluate the reflection phenomenon at the junction is to use the classical Goos–Hanchen theory for the collimated light reflection at interfaces, as in [14]. However, the refractive indexes in the cross section resemble a graded distribution due to the thermal expansion. It is difficult to find a precise analytical solution for the mode profile. As an approximation, we assume a parabolic indexes distribution as

$$n(x) = 1 - \frac{1}{2} a^2 (x - x_0)^2 \tag{5}$$

x is the direction vertical to the input waveguides in the waveguide plane, x_0 is the mode center, and a is the fitting coefficient. Using the Gauss–Hermite polynomials, the fundamental mode profile is [15]

$$\psi(x) = \left(\frac{ka}{\pi}\right)^{\frac{1}{4}} \exp\left[-\frac{ka(x - x_0)^2}{2}\right] \tag{6}$$

where $k = 2\pi n/\lambda$ is the wavenumber in the optical media. Fig. 5(a) shows the fundamental mode profiles for different wavelengths, suggesting that longer wavelengths will result in larger mode diameters. Hence, the optical power leakage into the cross port will aggravate the excess loss and crosstalk, resulting in the bandwidth limitation of the TIR structure. If the wavelength is very short, higher order modes will dominate the

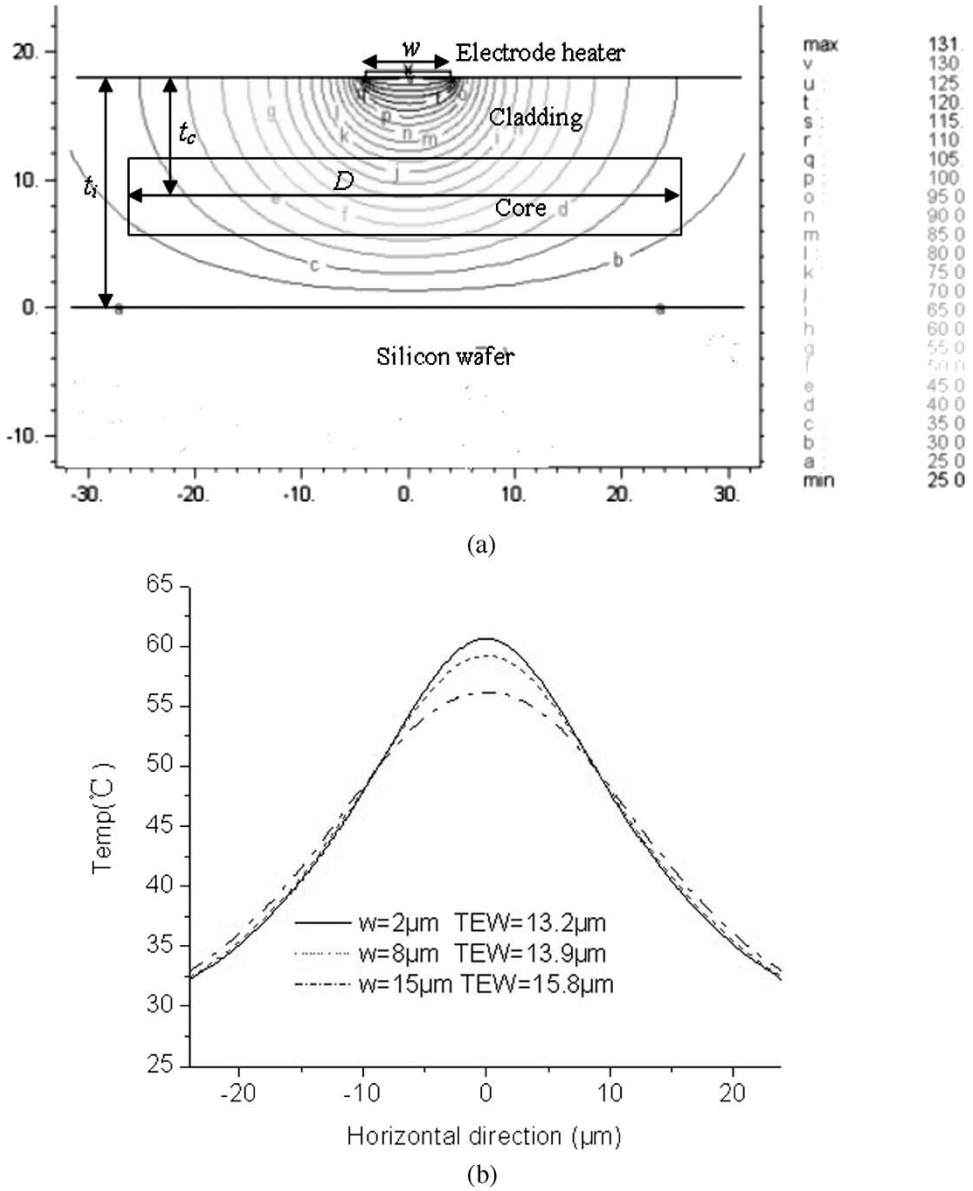

Fig. 3. Thermal steady state simulation for the active region (a) temperature contour map and (b) temperature distribution for different electrode width.

behavior, which will increase the radiation losses at the taper regions. Fig. 5(b) shows how the performances vary with λ by 2-D semi-vector beam propagation method (2-D SV BPM) simulations. If we require the excess loss to be less than 3 dB and crosstalk less than -25 dB, the expected bandwidth is 4200 nm ($0.6-4.8$ μm), which is much broader than any conventional optical switch structures based on beam interference.

III. Device Fabrication

ZPU12-RI series polymer materials with the TO coefficient of $-1.7 \times 10^{-4}/^{\circ}$C from Chemoptics are employed to make optical waveguides on silicon wafers. First, a layer of ZPU12-450 ($n = 1.45$) as the bottom cladding is spin coated onto the wafer. After UV and thermal curing, a second layer of ZPU12-460 ($n = 1.46$) is spun which servers as the core layer. A suitable thickness of a hard masking material is then deposited and patterned by either a wet or dry etching method. Silicon dioxide (SiO_2) is employed as the hard mask material because it has the ability to be dry etched with reactive ion etching (RIE) plasma. The dry etch process yields smoother hard mask edges compared with wet etching, thereby reducing the roughness of the polymer waveguide sidewalls, but the conventional plasma enhanced chemical vapor deposition (PECVD) process to grow SiO_2 requires a high temperature (285 °C), which is quite close to the polymer degradation point (300 °C). We developed a low temperature PECVD recipe running under 200 °C, which is quite close to the thermal baking temperature and will not cause undue material degradation loss. The measured propagation loss of the fabricated channel waveguide is 0.38 dB/cm at a 1.55 μm wavelength. This is close to the limit set by the material absorption, measured from the planar waveguide propagation loss, which is 0.35 dB/cm. Once the hard mask is properly defined, RIE is used to form the channel waveguides in the core material. The remaining hard mask is then removed by wet etching, and a polymer top cladding layer

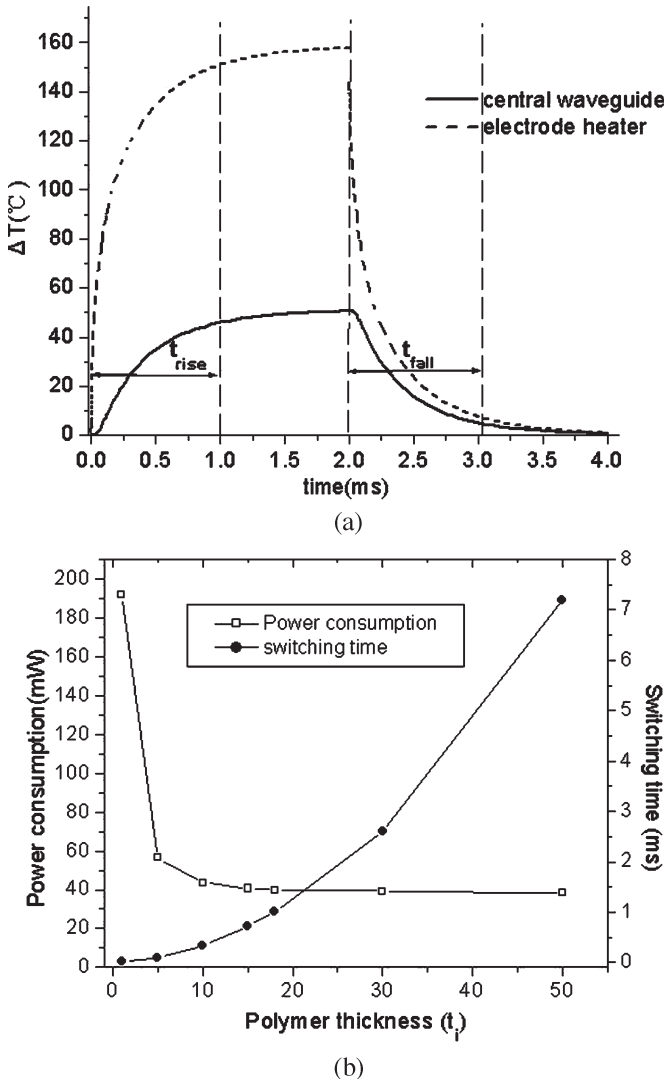

Fig. 4. Transient thermal state for the active region (a) time domain temperature cycle and (b) switching time and power consumption as functions of polymer thickness.

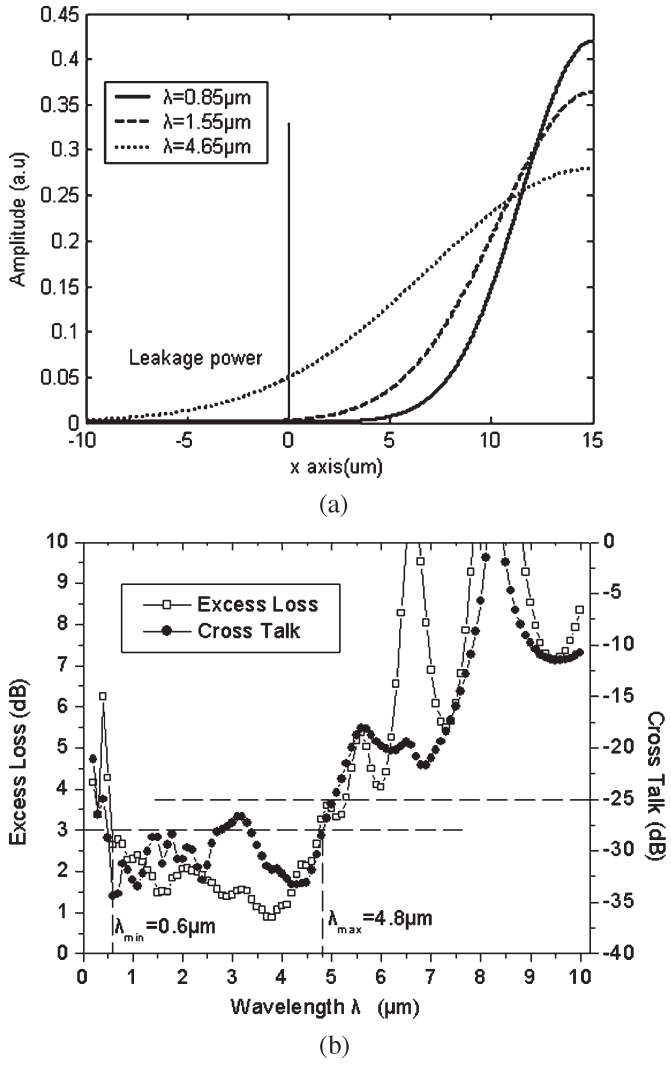

Fig. 5. (a) Fundamental mode profiles of different wavelengths and (b) simulated bandwidth of the TIR structure.

is spin coated and cured. Fig. 6 shows a part of the core layer in the junction with smooth sidewalls produced by the RIE process. Afterwards, a 300-nm gold film is deposited on the top cladding and patterned by photolithography. Wet etching is used to form the electrode heater. Fig. 7 shows the patterned electrode on top of the X junction. In the last step, the device is cleaved and the facets are polished to form a good coupling interface with a single mode fiber.

IV. Results and Discussion

A. Switching Characteristics

A Thorlabs amplified spontaneous emission filter lightsource (ASE-FL) 7001P broadband light source (1.53−1.61 μm) is used to launch the light through a single mode fiber into the optical switches. Fig. 8 shows the near field pattern of the TO switch in the cross and bar state, respectively. The mode profiles are composed of the fundamental modes with a separation of 250 μm.

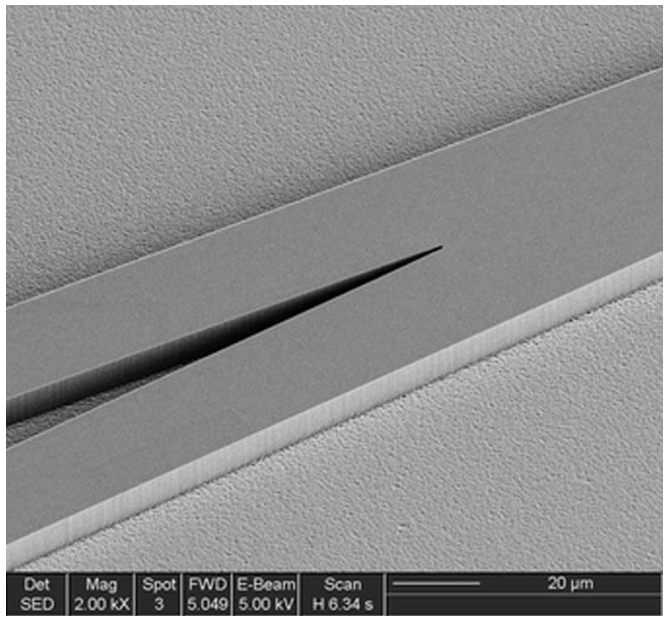

Fig. 6. Scanning electron microscope (SEM) of the core at the junction.

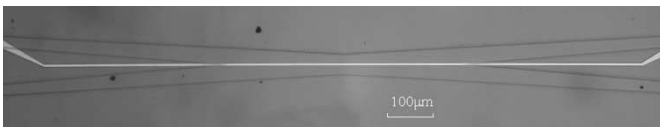

Fig. 7. X junction with electrode heater.

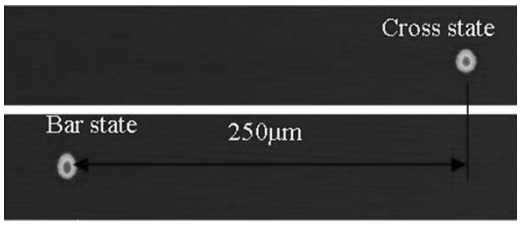

Fig. 8. Near field patterns in cross and bar state.

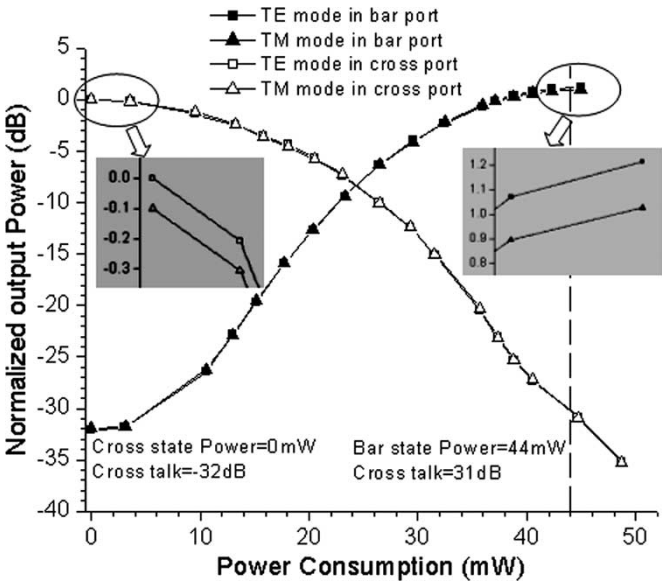

Fig. 9. Switching characteristics of the TIR switch.

Fig. 9 shows the optical power of the TE and TM modes in the cross port and the bar port responding to the driving power. The tested switch, with a half branch angle of 4°, has a crosstalk of −32 dB in the cross state and a power consumption of 0 mW. The zero static power consumption is a profitable feature since it can reduce the average driving power in real applications. With a driving power increase, the optical power in the cross port will decrease but in the bar port will increase simultaneously. Eventually, the switch will reach the bar state. In this paper, we define the driving power resulting in maximum optical power in the bar port as the bar state power consumption, which is 44 mW in Fig. 9, achieving a crosstalk of −31 dB. The TE and TM modes show almost the same response to the driving power. The PDL is 0.1 dB in the cross state and 0.2 dB in the bar state. The measured total resistance including the pads and lead lines is 48.0 Ω and the resistance of the heater is 39.1 Ω so that the thermal efficiency is estimated to be 81.5%.

The performance of the TIR switches for different values of θ is listed in Table I.

TABLE I
PERFORMANCE OF THE TIR SWITCHES WITH DIFFERENT θ

θ (degree)	3	4	5
Effective Length(μm)	5294	4274	3731
Cross talk in cross state(dB)	-20	-31	-40
Cross talk in bar state(dB)	-23	-32	-41
Excess loss in the cross state(dB)	1.3	0.9	1.4
Excess loss in the bar state(dB)	0.95	0.62	1.15
Switching Power (mW)	25	44	66

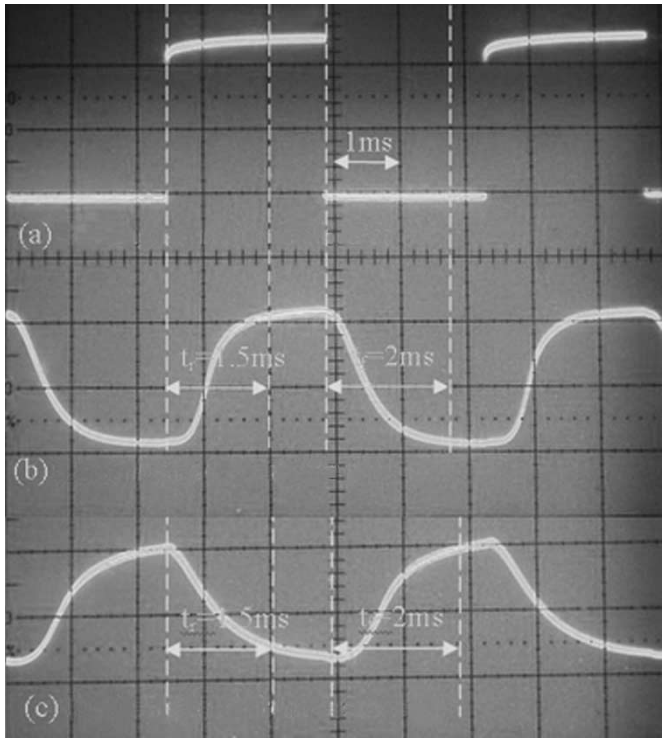

Fig. 10. Dynamic response of the optical signal to the driving signal. (a) Driving signal to the heater. (b) Optical signal from bar port. (c) Optical signal from cross port.

For practical applications, the fiber-to-fiber insertion loss is more important than the excess loss. We shortened the input/output waveguide to reduce the propagation loss. With a total device length of 19 mm, the lowest insertion loss we have achieved is 2.8 dB.

B. Switching Time

The switching time of the TIR switch is determined by the thermal conductivity and thickness of the polymer, but for the loss issue (thinner polymer layer results in larger metal and substrate absorption), the total thickness is still around 18 μm. Both our simulation and experimental results show that the switching time of the TIR TO switch is independent of the geometric parameters of the X junction. We used a 200-Hz square waveform with an amplitude of 1.3 V and an offset at 0.65 V to drive the heater of the switch with a half branch angle of 4°. The dynamic power consumption is calculated to be 43.2 mW, which is very close to the value in Table I. The optical response in the two output channels, as shown in Fig. 10, demonstrates a delay of 1.5 ms for $t_{\rm rise}$ and 2 ms for $t_{\rm fall}$. The

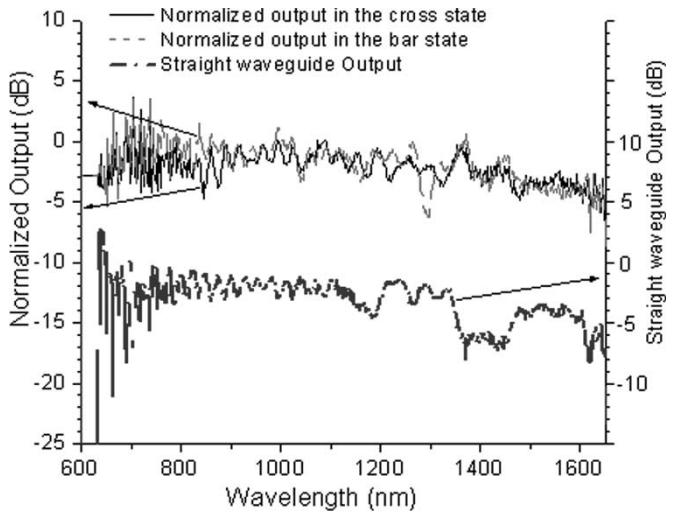

Fig. 11. Optical response as a function of the wavelength.

measured speed is a little bit slower than the simulation results (1 ms for $t_{\rm rise}$ and 1.1 ms for $t_{\rm fall}$), which is possibly caused by the approximation of the 2-D FEA model.

C. Optical Bandwidth

The fabricated devices have good performance over the wavelengths from $1.53-1.61$ μm as described in Section IV-A and B. To find the bandwidth limit, a white light source (AQ 4303-B) is used as the broadband supply. The bandwidth of the white light source covers from 400–1800 nm. The output optical power is measured by a spectrum analyzer (ANDO AQ6317B), having a response to wavelengths between 600 and 1800 nm. The throughput of a straight waveguide with the same length as the optical switch is first monitored, as shown in Fig. 11. If the wavelength is smaller than 630 nm, the throughput is below the sensitivity of the spectrum analyzer due to the large material absorption. From 630 to 850 nm, the throughput shows a rapid and large variation, indicating that the propagation loss is sensitive to the wavelength. This situation became much worse when the wavelength is larger than 1650 nm, which is not shown in Fig. 11 for clarity. In order to evaluate the optical bandwidth excluding the impact of material absorption, the output power of the TIR optical switch in the cross and bar state is normalized to the throughput of the straight waveguide. The results are also shown in Fig. 11, indicating that the optical switch has a very uniform output in the cross and bar state at the wavelength range of $850 \sim 1630$ nm. If the wavelength is smaller than 850 nm, the measurement errors become bigger due to the material loss sensitivity. The performance beyond 1630 nm is not determinable because of the rapid oscillation. We cannot confirm the ideal structure-limited bandwidth of the optical switch based on our experiments. However, our fabricated TIR optical switches can work over the wavelength range from 630 to 1630 nm.

V. Conclusion

We proposed the optimal design for a 2×2 TO switch using TIR effects. The geometric parameters of the X junction which will affect the excess loss and crosstalk were optimized, and the thermal characteristics with relation to the electrode heater width and polymer thickness were studied as well. In order to decrease the power consumption, the heater length was shortened, and also a taper structure was introduced to the lead electrodes to reduce the power consumption beyond the X junction. The reflection at the junction is simulated by incorporating the horizontal index distribution, which was caused by a temperature gradient, into the junction. This showed that the reflection was not sensitive to the wavelength. Thus, the TIR structure can achieve a large optical bandwidth.

The fabrication procedures were also optimized by using a layer of RIE patterned SiO_2, which was grown by PECVD at a low temperature. The waveguide loss was successfully reduced to 0.38 dB/cm. We fabricated TIR TO switches with half branch angle of 3°, 4°, and 5°. The measured excess loss was slightly different, from which may have been caused by fabrication and measurement factors. The shortened devices also showed low fiber-to-fiber insertion losses at 2.8 dB, which is 8.4 dB lower than [7], and 1.2 dB lower than [8]. This improvement is attributed to adopting the better polymer material and the optimal structure and fabrication procedure. By increasing the half branch angle, the effective length will decrease, and the crosstalk will be greatly improved. As a tradeoff, we have to provide more driving power, but this is still a low power consumption ($<$ 66 mW) due to the improved heater design. The switching time, which is independent of the half branch angle, is 1.5 ms in rising time and 2 ms in falling.

As an emphasis, the biggest achievement of the optical switches was their low PDL (0.2 dB) and broad optical bandwidth. These features can make them suitable for applications, such as board-level optical interconnects, local area networks, long haul communication, and optical true time delay.

References

[1] M. Okuno, "Highly integrated PLC-type optical switches for OADM and OXC systems," in *Proc. Optical Fiber Communications Conf.*, Atlanta, GA, Mar. 2003, vol. 1, pp. 169–170.

[2] K. Horikawa, I. Ogawa, H. Ogawa, and T. Kitoh, "Photonic switched true time delay beam forming network integrated on silica waveguide circuits," in *Proc. IEEE MTT-S Int. Microwave Symp. Dig.*, Orlando, FL, 1995, vol. 1, pp. 65–68.

[3] J. D. Shin, B. S. Lee, and B. G. Kim, "Optical true time-delay feeder for X-band phased array antennas composed of 2×2 optical MEMS switches and fiber delay lines," *IEEE Photon. Technol. Lett.*, vol. 16, no. 5, pp. 1364–1366, May 2004.

[4] L. Eldada, "The promise of polymers," *SPIE's OEmagazine*, vol. 2, no. 5, pp. 26–29, May 2002.

[5] C. S. Tsai, B. Kim, and F. R. El-Akkari, "Optical channel waveguide switch and coupler using total internal reflection," *IEEE J. Quantum Electron.*, vol. QE-14, no. 7, pp. 513–517, Jul. 1978.

[6] J. Yang, Q. Zhou, and R. T. Chen, "Polyimide-waveguide-based optical switch using total-internal-reflection effect," *Appl. Phys. Lett.*, vol. 81, no. 16, pp. 2947–2949, Oct. 2002.

[7] X. Wang, B. Howley, M. Chen *et al.*, "Polymer based thermo-optic switch for optical true time delay," in *Proc. SPIE—Photonics West*, San Jose, CA, Jan. 2005, vol. 5728, pp. 60–67.

[8] Y. Silberberg, P. Perimutter, and J. E. Baran, "Digital optical switch," *Appl. Phys. Lett.*, vol. 51, no. 16, pp. 1230–1232, Oct. 1987.

[9] Q. Lai, W. Hunziker, and H. Melchior, "Low-power compact 2×2 thermooptic silica-on-silicon waveguide switch with fast response," *IEEE Photon. Technol. Lett.*, vol. 10, no. 5, pp. 681–683, May 1998.

[10] H. Kogelnik and R. V. Schmidt, "Switched directional couplers with alternating $\Delta\beta$," *IEEE J. Quantum Electron.*, vol. QE-12, no. 7, pp. 396–401, Jul. 1976.

[11] P. C. Lee and E. Voges, "Three-dimensional semi-vectorial wide-angle beam propagation method," *J. Lightw. Technol.*, vol. 12, no. 2, pp. 215–225, Feb. 1994.
[12] C. Lee, M. Wu, L. Sheu, P. Fan, and J. Hsu, "Design and analysis of completely adiabatic tapered waveguides by conformal mapping," *J. Lightw. Technol.*, vol. 15, no. 2, pp. 403–410, Feb. 1997.
[13] H. A. Schafft, "Thermal analysis of electro-migration test structures," *IEEE Trans. Electron Devices*, vol. ED-34, no. 3, pp. 664–672, Mar. 1987.
[14] I. Cayrefourcq, M. Schaller, C. Fourdin *et al.*, "Optical switch design for true time delay array antenna," *Proc. Inst. Elect. Eng.—Optoelectron.*, vol. 145, no. 1, pp. 77–82, Feb. 1998.
[15] C. C. Constantinou and R. C. Jones, "Path integral analysis of the linearly tapered graded-index waveguide," *J. Phys. D, Appl. Phys.*, vol. 24, no. 6, pp. 839–848, Jun. 1991.

Xiaolong Wang received the B.S. degree in material science and engineering from Tsinghua University, Beijing, China, and the M.S. degree in electrical engineering from the Chinese Academy of Sciences, Beijing, in 2000 and 2003, respectively. Since 2003, he has been working toward the Ph.D. degree in electrical engineering at the University of Texas at Austin.

From 2000 to 2003, his research topic was silicon-based photonic devices for high-speed communication system. His current research include polymeric photonic devices for true time delay (TTD) and board-level optical interconnects.

Brie Howley received the B.S. degree from the University of Wisconsin–Madison in 1998. Since 2001, he has been working toward the Ph.D. degree in electrical engineering in the areas of plasma, optics, and quantum electronics at the University of Texas at Austin.

From 1998 to 2001, he worked for Motorola's Semiconductor Product Sector in the discrete components research and development team. His research topic is optically controlled, wide bandwidth phased array antennas (PAAs).

Maggie Y. Chen (M'03) received the Ph.D. degree in electrical engineering in optoelectronic interconnects in 2002 from the University of Texas at Austin.

Her research work in the past ten years has been focused on optical TTD feeding networks for phased-array antennas, planar waveguide devices, optoelectronic interconnects, and diffractive optical elements. She has served as Principal Investigator for projects from National Science Foundation (NSF), Missile Defense Agency (MDA) and Commander, Space and Naval Warfare Systems Command (SPAWAR), Defense Advanced Research Projects Agency (DARPA), and National Aeronautics and Space Administration (NASA). She has over 30 publications in refereed journals and conferences.

Ray T. Chen (M'91–SM'98–F'04) received the B.S. degree in physics from the National Tsinghua University, Hsinchu, Taiwan, R.O.C., in 1980 and the M.S. degree in physics and the Ph.D. degree in electrical engineering, in 1983 and 1988, respectively, from the University of California.

He is the Temple Foundation Endowed Professor at the University of Texas (UT) at Austin. He joined the UT Austin as a member of the faculty to start optical interconnect research program in the ECE Department in 1992. Prior to his UT professorship, he worked as a Research Scientist, Manager, and Director of the Department of Electrooptic Engineering in Physical Optics Corporation, Torrance, CA, from 1988 to 1992. He also served as the CTO/Founder and Chairman of the Board of Radiant Research from 2000 to 2001, where he raised $18 million in A-Round funding to commercialize polymer-based photonic devices. His research work has been awarded more than 80 research grants and contracts from sponsors such as Department of Defense (DOD), National Science Foundation (NSF), Department of Energy (DOE), NASA, the State of Texas, and private industry. His research topics are focused on two main subjects: polymer-based guided-wave optical interconnection and packaging and TTD wideband PAA. Experiences garnered through these programs in polymeric material processing and device integration are pivotal elements for the research work reported herein. His group at UT Austin has reported its research findings in more than 400 published papers, including over 55 invited papers. He holds 12 issued patents. There are 23 students who received the EE Ph.D. degree from his research group at UT Austin. He has served as an Editor or Coeditor for 18 conference proceedings. He has also served as a Consultant for various federal agencies and private companies and delivered numerous invited talks to professional societies.

Dr. Chen is a Fellow of Optical Society of America (OSA) and The International Society of Optical Engineering (SPIE). He was the recipient of the 1987 UC Regent's dissertation fellowship and the 1999 UT Engineering Foundation Faculty Award for his contributions in research, teaching, and services. In his undergraduate years at the National Tsinghua University, he led a university debate team in 1979, which received the national championship of the national debate contest in Taiwan. He has chaired or been a program committee member for more than 50 domestic and international conferences organized by IEEE, SPIE, OSA, and the Photonics Society of Chinese-Americans (PSC).